ROYAL SOCIETY
OF CHEMISTRY

PAPER

Check for updates

Hydroxyl radical generation in peroxymonocarbonate/Co^{2+} systems: kinetic and mechanistic insights

Thi Tinh Vu, [ID] [a] Ngoc Duy Vu [ID] [b] and Thi Bich Viet Nguyen [ID] *[a]

This study investigates the generation of hydroxyl radicals ($^{\bullet}$OH) in a peroxymonocarbonate (PMC)-based advanced oxidation process (AOP) catalyzed by Co^{2+}. Steady-state $^{\bullet}$OH concentrations ([$^{\bullet}$OH]$_{ss}$) were quantified using terephthalic acid (TA) as a probe. The presence of PMC alone had negligible effect on $^{\bullet}$OH production, whereas Co^{2+} markedly enhanced radical formation. Specifically, [$^{\bullet}$OH]$_{ss}$ increased from 4.03×10^{-17} M in the H$_2$O$_2$-only system to 2.25×10^{-16} M in H$_2$O$_2$ + Co^{2+}, and from 2.26×10^{-17} M in PMC-only to 3.38×10^{-16} M in PMC/Co^{2+}. This enhancement is attributed to a Fenton-like mechanism involving Co^{2+}. Kinetic analysis revealed first-order dependence on TA concentration ($R^2 \approx 0.99$), Langmuir-type dependence on PMC concentration, and linear correlation with Co^{2+} concentration. Inorganic anions exhibited diverse roles, with Cl$^-$ enhancing $^{\bullet}$OH generation by ~26%, whereas SO$_4^{2-}$ and HPO$_4^{2-}$ suppressed it by ~35 and ~25%, respectively. A kinetic model describing radical generation agreed well with experimental data, offering valuable mechanistic insights and highlighting practical applicability of PMC-based AOPs for controlled $^{\bullet}$OH generation.

1 Introduction

Advanced oxidation processes (AOPs) have been extensively developed as powerful technologies for the degradation of refractory organic contaminants in water and wastewater treatment. Typical AOPs include the Fenton and Fenton-like systems,[1] ozonation,[2] photocatalysis,[3] persulfate activation,[4] and more recently peroxymonocarbonate-based oxidation systems.[5] Peroxymonocarbonate (HCO$_4^-$, PMC) is a highly reactive oxidising species that can be generated *in situ* by the reaction of hydrogen peroxide (H$_2$O$_2$) with bicarbonate (HCO$_3^-$), carbonate (CO$_3^{2-}$), or dissolved CO$_2$. This system is especially attractive because both HCO$_3^-$ and H$_2$O$_2$ are environmentally benign and readily available, making PMC-based systems a promising option for advanced oxidation processes (AOPs). The presence of transition metal ions, such as Co^{2+}, Fe^{2+}, or Cu^{2+}, in small amounts can further enhance PMC formation,[5,6] leading to a cascade of reactive oxygen species (ROS). Reported ROSs in the PMC-related reactions include the hydroxyl radical ($^{\bullet}$OH), superoxide anion radical (O$_2^{\bullet-}$), hydroperoxyl radical (HO$_2^{\bullet}$), singlet oxygen (^{1}O$_2$), bicarbonate radical (HCO$_3^{\bullet}$), and carbonate anion radical (CO$_3^{\bullet-}$).[7–9] Each of these reactive species contributes differently to the oxidative capacity of the system, but the $^{\bullet}$OH radical is regarded as the most

powerful due to its high redox potential and extremely high reactivity toward a broad spectrum of organic pollutants. The $^{\bullet}$OH radical has standard redox potentials of +2.8 V in acidic media, +1.8 V at neutral pH, and +1.55 V under alkaline conditions. Such values explain its ability to rapidly oxidise most organic molecules through electron transfer, hydrogen atom abstraction, or electrophilic addition to unsaturated bonds and aromatic systems. Its reaction rate constants with organic compounds typically fall in the range of 10^8 to 10^{10} (M^{-1} s^{-1}),[10,11] underscoring both its non-selectivity and high efficiency. Because of these properties, $^{\bullet}$OH is considered a central oxidant in many AOPs, such as Fenton chemistry, photocatalysis, ozonation, and peroxone processes. However, despite its importance, $^{\bullet}$OH detection and quantification remain a significant challenge due to its extremely short lifetime (~10^{-9} s) and low steady-state concentrations in aqueous solutions.

As other transient species, $^{\bullet}$OH radical can only be analysed by fast reaction techniques such as pulse methods, which determine absolute rate constants from reactant decay or product growth, or relative rate constants *via* competition methods. In principle, $^{\bullet}$OH radicals can be quantitatively analysed by both direct and indirect methods.[11,12] Direct detection techniques, such as electron spin resonance (ESR) can provide conclusive evidence of $^{\bullet}$OH formation, since ESR generates characteristic spectra for radical species. Yet, ESR detection of $^{\bullet}$OH is hampered by its weak signals, requiring the use of spin-trapping agents, such as 5,5-dimethyl-1-pyrroline *N*-oxide, 5-*tert*-butoxycarbonyl-5-methyl-1-pyrroline *N*-oxide, 5-di-ethoxyphosphoryl-5-methyl-1-pyrroline-*N*-oxide.[13] These agents

[a]Faculty of Chemistry, Hanoi National University of Education, 136 Xuan Thuy Str., Hanoi, Vietnam. E-mail: vietntb@hnue.edu.vn

[b]Faculty of Chemistry, VNU University of Science, Vietnam National University Hanoi, 19 Le Thanh Tong str., Hanoi, Vietnam

react with 'OH radical to form more stable radical adducts that enhance ESR sensitivity.

Indirect methods, which are more widely used, rely on rapid reactions of 'OH with probe molecules. In this approach, changes in probe concentration or product accumulation are monitored, from which the steady-state concentration of 'OH can be deduced. Numerous compounds have been used for 'OH probing, such as 1,2-benzopyrone (coumarin),[14] hydroxymethanesulfonate,[15] dimethylsulfoxide,[16] benzene,[17] nitrobenzene,[18] benzoic acid,[19] salicylate,[20] phenylalanine,[21] phthalic hydrazide,[22] p-chlorobenzoic acid,[23] terephthalic acid,[24–27] etc. However, each probe comes with certain limitations, such as multiple reaction pathways, non-specific products, or interference from other ROS. When using non-aromatic probe compounds, 'OH may attack different positions on the target molecule to form a group of products, which may give uncertainty in quantifying formed species. Regarding aromatic compounds, 'OH predominantly reacts with the ring, not with substituents. Therefore, aromatic substances are preferentially selected.

Among available aromatic probes, terephthalic acid (TA) has emerged as one of the most reliable for 'OH quantification due to its selective reaction with this radical to form a hydroxylated product, as depicted in the following pathway (Fig. 1).

TA itself is non-fluorescent, but upon hydroxylation by 'OH it yields a single product, 2-hydroxyterephthalate (hTA), which is both highly stable and strongly fluorescent. This one-to-one stoichiometry between 'OH and hTA, coupled with the high sensitivity of fluorescence spectroscopy, enables accurate, selective, and cost-effective measurement of 'OH even at very low concentrations. For these reasons, TA has become increasingly popular for 'OH detection in complex aqueous systems.

Despite the extensive body of literature on hydroxyl radicals in AOPs,[10–27] studies focusing specifically on their role in peroxymonocarbonate-driven systems remain limited. Previous works, including our studies on dye degradation, have suggested that carbonate radicals are often the dominant oxidants in PMC systems, while hydroxyl radicals appear to play a comparatively minor role. This observation may be attributed to the much lower concentrations and shorter lifetime of 'OH radical compared to $CO_3^{\bullet-}$.[28] However, a systematic and quantitative investigation of 'OH in PMC/metal ion systems has yet to be carried out. Such information is essential for developing a clearer mechanistic understanding of PMC-based oxidation and for guiding the rational design of more efficient AOPs.
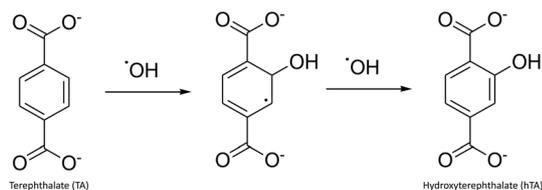
Therefore, in this study, we aim to quantify the 'OH radicals generated in aqueous PMC/Co^{2+} systems using TA as a selective fluorescent probe. The steady-state concentration of 'OH is determined under varying experimental conditions in order to assess the influence of different system components. Furthermore, a kinetic model is established to describe the relationship between these components and 'OH generation, providing new mechanistic insights into the role of hydroxyl radicals in PMC-mediated oxidation processes.

2 Materials and methods

2.1. Materials

All chemicals, including terephthalic acid (TA), 2-hydroxyterephthalic acid (hTA), sodium bicarbonate, hydrogen peroxide, sodium hydroxide, and cobalt(II) nitrate, were of analytical grade and purchased from Sigma-Aldrich.

2.2. Fluorescence measurements

The hTA concentration at time t was monitored by measuring hTA fluorescence at excitation and emission wavelengths of 310 nm and 425 nm, respectively, using a PerkinElmer FL 8500 fluorescence spectrophotometer. The hTA concentration was determined using the standard curve $I_{em} = (29\,212 \pm 96)$. C_{hTA} (μM) + (83.5 ± 62.4) ($R^2 = 0.99998$) in a linear range of 0.06–1.20 μM with the LOD and LOQ of 6.4 nM and 21.3 nM, respectively (see SI.2. for detailed method validation).

2.3. Investigating the factors influencing the 'OH formation

The influence of various reaction parameters on the 'OH formation was examined according to the conditions summarised in Table 1. The investigated factors included: (i) oxidation system composition (trials 1 ÷ 5, 8), (ii) TA concentration (trials 6 ÷ 12), (iii) HCO_4^- concentration (trials 13 ÷ 18), and (iv) Co^{2+} catalyst concentration (trials 19 ÷ 23). For trials 2 ÷ 20, the HCO_3^- : H_2O_2 mixture (molar ratio 1 : 2.5) was prepared 50 minutes prior to the addition of Co^{2+} catalyst and TA solution.

All experiments were conducted in a 50-mL batch reactor under continuous magnetic stirring at 25 ± 1 °C. At predetermined time intervals, aliquots were withdrawn and analysed for fluorescence ($\lambda_{em} = 425$ nm at $\lambda_{ex} = 310$ nm) to quantify hTA formation. Each experimental condition was performed in triplicate to ensure reliability and reproducibility.

2.4. Experimental method for determining 'OH concentration

The second-order kinetic law of the reaction between 'OH and terephthalic acid (TA) is given by eqn (1):

$$r = \frac{d[hTA]}{dt} = k_{\cdot OH\text{-}TA}[{}^{\bullet}OH][TA] \tag{1}$$

The second-order rate constant, $k_{\cdot OH\text{-}TA}$, was previously determined to be 4.4×10^9 M^{-1} s^{-1}.[24]

During the reaction, the 'OH concentration is assumed to be in steady state; therefore, eqn (1) can be written as:

Fig. 1 The hydroxylation of TA by 'OH radicals to form fluorescent hTA.

Table 1 Experimental conditions for hTA formation

Trial	$[HCO_3^-]$ mM	$[H_2O_2]$ mM	$[Co^{2+}]$ μM	$[TA]$ mM	pH[a]
1	0	10	0	0.048	7
2	4	0	0	0.048	9
3	0	10	0.68	0.048	7
4	4	0	0.68	0.048	9
5	4	10	0	0.048	9
6 ÷ 12	4	10	0.68	0.006; 0.012; 0.048; 0.072; 0.090; 0.120; 0.150	9
13 ÷ 18	0.4; 1; 2; 4; 6; 8	1; 2.5; 5; 10; 15; 20	0.68	0.048	9
19 ÷ 23	4	10	0.34; 0.68; 1.36; 1.70; 3.39	0.048	9

[a] A preliminary study was conducted to investigate the influence of pH conditions on hTA fluorescence, which indicated that hTA fluorescence appeared to be stable in a wide range of pH, from 5 to 12.

$$r = \frac{d[hTA]}{dt} = k'_{OH\text{-}TA}[TA] \qquad (2)$$

where $k'_{OH\text{-}TA}$ is the *pseudo* first-order rate constant, $k'_{OH\text{-}TA} = k_{OH\text{-}TA}['OH]$.

During the initial stage of the reaction, the TA concentration changes negligibly and can thus be regarded as constant. Eqn (2) is then integrated to obtain eqn (3):

$$[hTA] = k'_{OH\text{-}TA}[TA]t \qquad (3)$$

The product $k'_{OH\text{-}TA}[TA]$ can be obtained from the slope of the plot of [hTA] *versus* time (t). From this, both $k'_{OH\text{-}TA}$ and the steady-state concentration of 'OH can be determined.

3 Results and discussions

3.1. 'OH formation in the absence of PMC

Fluorescence spectra of TA-containing solutions with different compositions are presented in Fig. 2. In systems where PMC was not generated (trials 1 ÷ 5, Fig. 2a–d), no fluorescence signal was detected in the absence of H_2O_2 (Fig. 2a and c), indicating that no 'OH radicals were formed under these conditions. Importantly, hTA is a strong fluorophore with a high relative quantum yield of 63% compared to quinine sulfate (SI.1), ensuring high sensitivity of the applied analysis method.

By contrast, in the presence of H_2O_2 (Fig. 2b and d), the fluorescence intensity increased with reaction time, indicating a strong increase in 'OH concentration, especially when catalyzed by Co^{2+}. A kinetic investigation of the hTA formation revealed 'OH steady-state concentrations of 4.03×10^{-17} M for the 10 mM H_2O_2 solution and 2.25×10^{-16} M for the 10 mM $H_2O_2 + 0.68$ μM Co^{2+} solution (Table 2).

The findings suggest that 'OH radicals are formed through the decomposition of H_2O_2, which proceeds slowly in the absence of catalysts but is markerdly accelerated in the presence of Co^{2+} *via* the reactions as follows:

$$H_2O_2 \rightarrow 2'OH \qquad (R1)$$

$$H_2O_2 + Co^{2+} \rightarrow {}^{\cdot}OH + Co^{3+} + HO^- \qquad (R2)$$

Co^{3+} is then reduced back to Co^{2+} by H_2O_2:

$$H_2O_2 + Co^{3+} \rightarrow HO_2^{\cdot} + Co^{2+} + H^+ \qquad (R3)$$

These results highlight the catalytic role of Co^{2+} in accelerating 'OH generation. The underlying mechanism is consistent with a Fenton-like reaction, where Co^{2+} activates H_2O_2 to yield 'OH radicals (R2). Such Fenton-type chemistry is widely recognized in AOPs and explains the observed enhancement of 'OH formation in the presence of Co^{2+}.[11,29]

3.2. 'OH formation in the presence of PMC

It can be concluded from the comparison between Fig. 2b and e, Fig. 2d and f that the presence of bicarbonate and the consequent formation of PMC had only a negligible effect on 'OH generation, regardless of the presence of Co^{2+} catalyst. Specifically, the steady-state 'OH concentrations obtained for the 10 mM H_2O_2 solution and for the 4 mM $HCO_3^- + 10$ mM H_2O_2 solution were of the same order of magnitude, indicating that bicarbonate itself does not significantly alter the decomposition pathway of H_2O_2 under these conditions. By contrast, the addition of Co^{2+} dramatically enhanced 'OH production. In the PMC system catalyzed by Co^{2+}, fluorescence signals increased sharply with reaction time, corresponding to a nearly 10-fold higher 'OH concentration compared to the H_2O_2-only system and the PMC system without Co^{2+} (Table 2). This observation highlights the crucial catalytic role of Co^{2+} in activating PMC and H_2O_2, leading to efficient radical generation. The enhanced radical yield can be attributed to reactions such as:

$$HCO_4^- + Co^{2+} \rightarrow {}^{\cdot}OH + Co^{3+} + CO_3^{2-} \qquad (R4)$$

In this pathway, Co^{2+} acts as an electron donor to PMC, producing 'OH radicals while being oxidized to Co^{3+}. The subsequent reduction of Co^{3+} by H_2O_2 regenerates Co^{2+} and sustains the catalytic cycle, resembling a Co^{2+}/H_2O_2 Fenton-like mechanism but mediated by PMC.

Thus, the PMC/Co^{2+} system provides a dual activation effect: (i) Co^{2+} catalytically enhances H_2O_2 decomposition, and (ii) Co^{2+} directly reacts with PMC to generate additional 'OH. The synergy between these pathways accounts for the markedly higher 'OH radical concentration observed, supporting the potential of PMC-based systems as efficient AOPs.

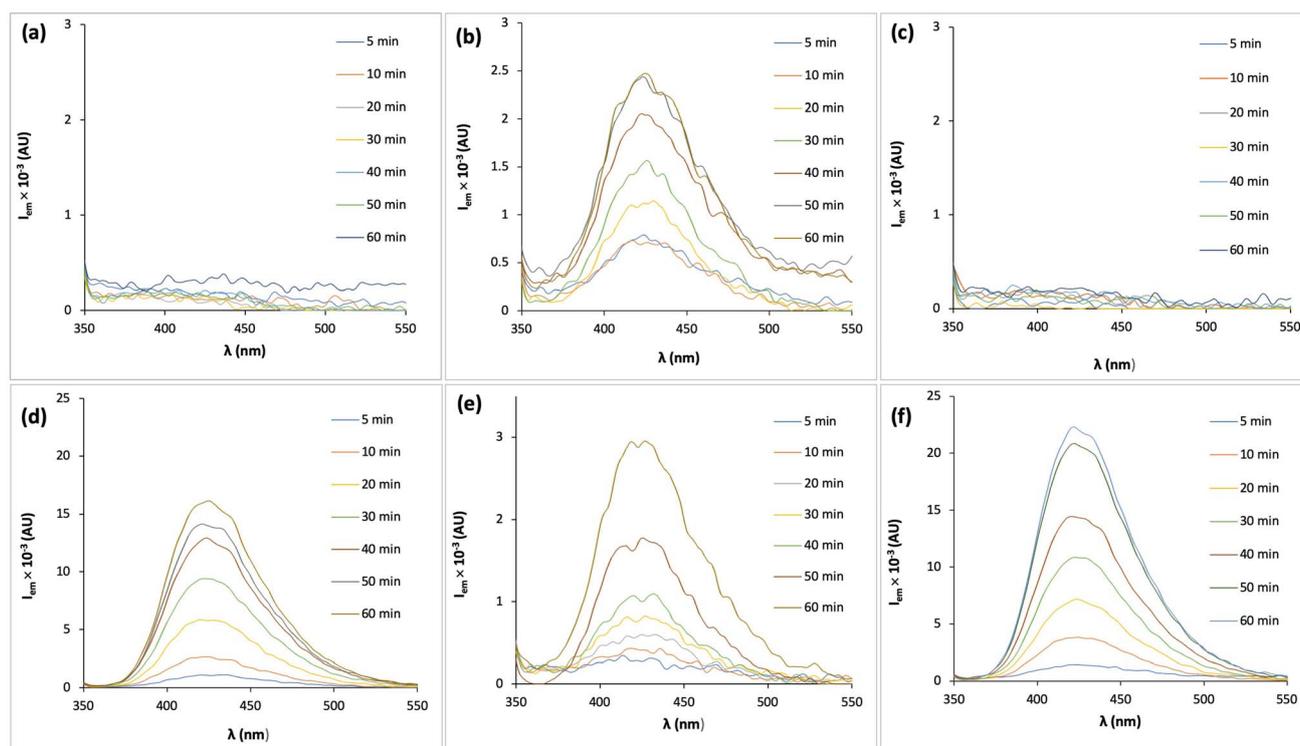**Fig. 2** Fluorescence spectra over time obtained for 0.048-mM TA solutions with varying solution compositions: (a) 4 mM HCO_3^-, (b) 10 mM H_2O_2, (c) 0.68 μM Co^{2+}, (d) 10 mM H_2O_2 + 0.68 μM Co^{2+}, (e) 4 mM HCO_3^- + 10 mM H_2O_2, (f) 4 mM HCO_3^- + 10 mM H_2O_2 + 0.68 μM Co^{2+}.

Table 2 $^•OH$ steady-state concentrations ($[^•OH]_{ss}$) determined for different reaction systems

Trial	Reaction systems	$[^•OH]_{ss} \times 10^{16}$, M
1	10 mM H_2O_2	0.40
3	10 mM H_2O_2 + 0.68 μM Co^{2+}	2.25
5	4 mM HCO_3^- + 10 mM H_2O_2	0.23
8	4 mM HCO_3^- + 10 mM H_2O_2 + 0.68 μM Co^{2+}	3.38

3.2.1. Effect of TA concentration. The kinetics of hTA formation in the PMC/Co^{2+} system at varying TA concentrations are shown in Fig. 3a, while the corresponding observed $^•OH$

steady-state concentration ($[^•OH]_{ss}$) derived from these kinetics are presented in Fig. 3b. As expected for a radical–probe interaction, the reaction rate increased proportionally with increasing TA concentration.

A linear relationship between $\ln(r)$ and $\ln([TA])$ with a correlation coefficient of $R^2 \approx 1$ (Fig. 3c) confirms that the reaction follows first-order kinetics with respect to TA concentration, consistent with the assumption made in the steady-state analysis. This strong linearity validates the use of TA as a quantitative probe for $^•OH$ detection in the PMC-based AOP systems.

Mechanistically, this observation indicates that $^•OH$ radicals generated in the PMC/Co^{2+} system react directly and efficiently with TA molecules without significant side reactions competing

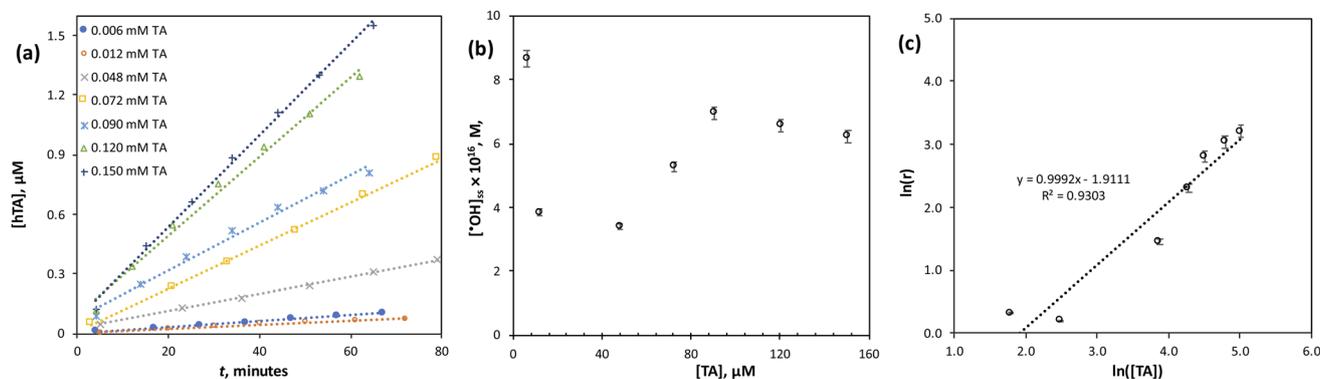**Fig. 3** (a) Kinetics of the hTA formation in the PMC/Co^{2+} system at different concentrations of TA: 4 mM HCO_3^-, 10 mM H_2O_2, 0.678 μM Co^{2+}, and TA in the range of 0.006–0.150 mM; (b) dependence of $[^•OH]_{ss}$ on the initial TA concentration; (c) linear dependence of $\ln(r)$ on $\ln([TA])$.

at the studied concentration range. The absence of deviation from first-order kinetics further suggests that radical recombination or scavenging by secondary species (*e.g.*, bicarbonate or carbonate) was negligible under the experimental conditions.

3.2.2. Effect of PMC oxidant concentration. The influence of PMC concentrations was investigated by varying the concentration of the $HCO_3^- : H_2O_2$ mixture as depicted in Fig. 4a and b. It can be observed that the $^\bullet OH$ concentration increased with increasing $HCO_3^- : H_2O_2$ concentration, which is expected since a higher precursor concentration promotes greater formation of PMC, thereby more $^\bullet OH$ generation in the system. However, the relationship between oxidant concentration and $^\bullet OH$ production was not linear but instead followed a saturation-type behavior well described by the Langmuir model (Fig. 4b). This indicates that beyond a certain point, further increases in oxidant concentration do not lead to linear increases in $^\bullet OH$ level. Mechanistically, this trend can be attributed to the coordination chemistry of Co^{2+}. At lower oxidant concentrations, additional $HCO_3^- : H_2O_2$ directly contributes to the formation of PMC, which reacts with Co^{2+} to generate reactive radicals reactions (R2) and (R4). However, at higher oxidant levels, excess oxidant species may saturate or partially inhibit the catalytic cycle through the formation of stable Co^{2+}-peroxo or Co^{2+}-carbonate complexes, reducing the availability of free Co^{2+} ions to continuously activate PMC. This is consistent with the Co^{2+}-complex formation theory, which predicts diminishing catalytic activity at elevated oxidant concentrations due to catalyst passivation.

This finding highlights the importance of optimizing oxidant dosage to balance radical production efficiency and catalyst utilization, a key principle in the design of advanced oxidation processes.

3.2.3. Effect of Co^{2+} catalyst concentration. The observed steady-state concentrations of $^\bullet OH$ radicals were derived from the kinetics of the hTA formation at various Co^{2+} concentrations, as shown in Fig. 5a and b. A clear linear dependence of $[^\bullet OH]_{ss}$ on Co^{2+} concentration was observed, indicating that

higher content of the catalyst proportionally accelerate radical formation. This result strongly supports the Co^{2+}-complex formation theory, which describes the activation of PMC through Co^{2+}-mediated redox cycle.

Mechanistically, the linearity suggests that Co^{2+} directly participates as the active catalytic center in the generation of $^\bullet OH$ radicals from PMC. In the absence of sufficient catalyst, the conversion of PMC to reactive radicals is limited; however, as Co^{2+} concentration increases, more active sites are available to drive the redox reaction, resulting in enhanced radical flux. This catalytic cycle can be expressed as shown in reaction (R4), followed by the regeneration of Co^{2+} *via* reactions with H_2O_2 or intermediate radical species.

Importantly, the observed linear trend implies that under the tested concentration range, catalyst deactivation or passivation by oxidant overloading (as seen in Section 3.2.2) is not yet significant. Therefore, the system is operating in a regime where radical formation efficiency is strongly catalyst-limited rather than oxidant-limited. This also suggests that optimizing Co^{2+} dosage is critical to maximize $^\bullet OH$ generation while minimizing excess use of oxidant precursors.

3.2.4. Effect of inorganic anions. The results in Fig. 6a and b demonstrate that the presence of inorganic anions can exert distinct effects on $^\bullet OH$ formation within the PMC/Co^{2+} system. Specifically, chloride (Cl^-) showed a positive effect (enhancement by 26%), sulfate (SO_4^{2-}) and hydrogen phosphate (HPO_4^{2-}) exerted inhibitory effects (reduction by 35% and 25%, respectively), while nitrate (NO_3^-) exhibited little or no impact.

The positive effect of chloride can be explained by its ability to interact with $^\bullet OH$ radicals, forming reactive chlorine species such as $Cl^\bullet$ and $Cl_2^{\bullet-}$.[11,30] These secondary oxidants, although less reactive than $^\bullet OH$, are longer-lived and can still contribute to pollutant degradation, thereby enhancing the apparent oxidation efficiency of the system.

In contrast, SO_4^{2-} and HPO_4^{2-} acted as scavengers of $^\bullet OH$ radicals, competing with the organic probe (TA) for reaction and consequently suppressing the observed $^\bullet OH$ concentrations.[31,32]
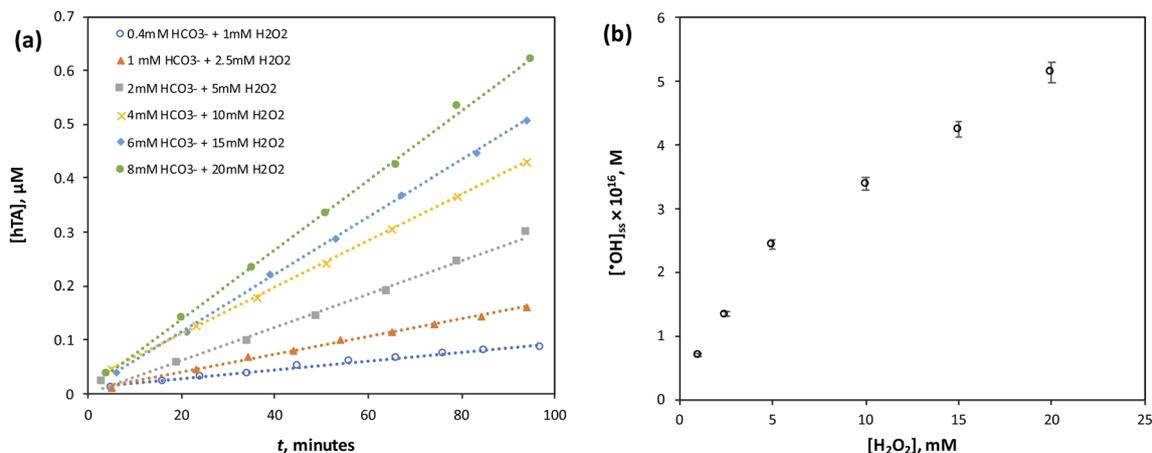

Fig. 4 (a) Kinetics of the hTA formation in the PMC/Co^{2+} system at different concentrations of oxidant: 0.048 mM TA, 0.68 μM Co^{2+}, and $HCO_3^- : H_2O_2$ at molar ratios of 0.4 : 1, 1 : 2.5, 2 : 5, 4 : 10, 6 : 15, 8 : 20 (mM); (b) dependence of observed $^\bullet OH$ concentration on the initial H_2O_2 concentration.
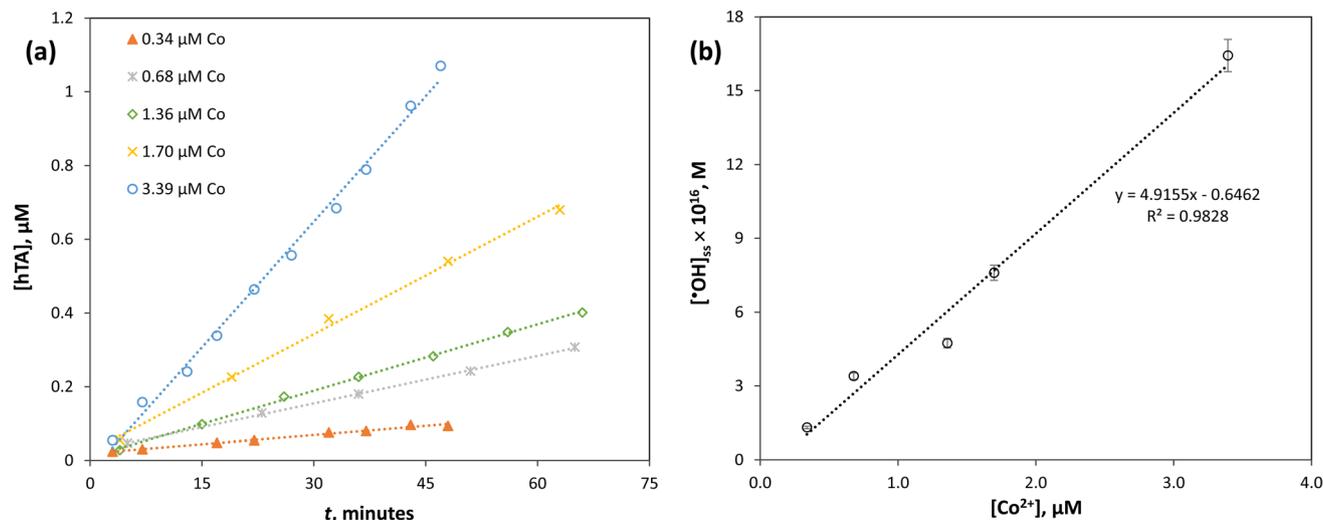
Fig. 5 (a) Kinetics of the hTA formation in the PMC/Co^{2+} system at different concentrations of Co^{2+} catalyst: 0.048 mM TA, 4 mM HCO_3^-, 10 mM H_2O_2, and Co^{2+} in the range of 0.34–3.39 μM; (b) dependence of observed $^•OH$ concentration on the Co^{2+} concentration.
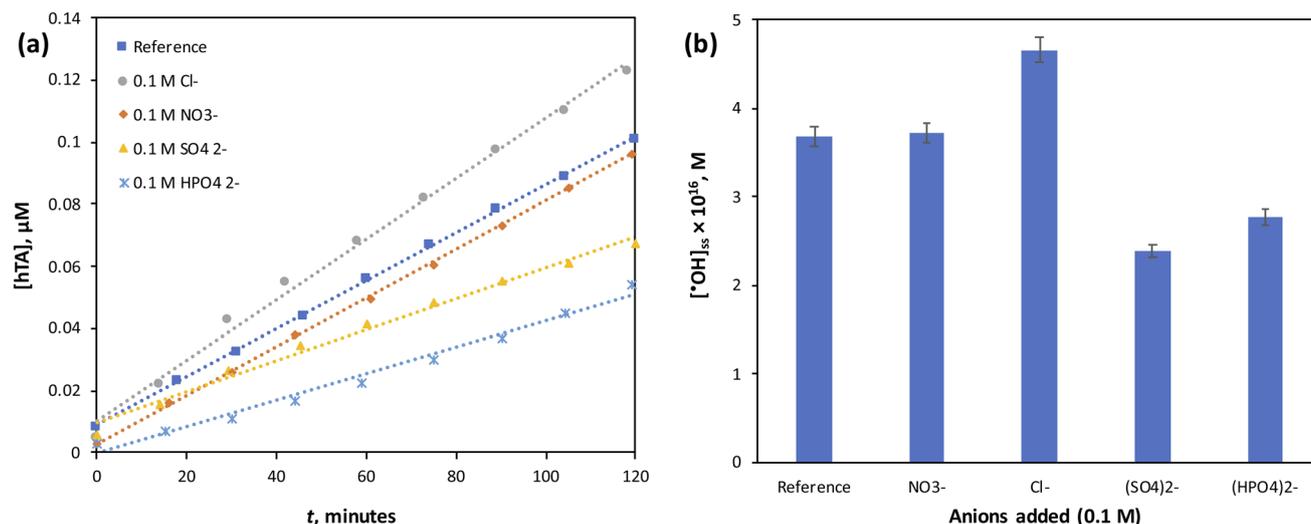

Fig. 6 (a) Kinetics of the hTA formation in the PMC/Co^{2+} system with various inorganic anions added: 0.048 mM TA, 4 mM HCO_3^-, 10 mM H_2O_2, 0.68 μM Co^{2+}, and various inorganic anions added at 100 mM concentration including NO_3^-, Cl^-, SO_4^{2-}, HPO_4^{2-}; (b) dependence of observed $^•OH$ concentration on the presence of inorganic anions added.

The neutral effect of NO_3^- may be attributed to its relatively low reactivity toward $^•OH$ under the tested conditions, as well as its inability to significantly complex with Co^{2+}.[31] Thus, nitrate does not interfere with either radical scavenging or catalyst activity, resulting in negligible impact on $^•OH$ formation.

Overall, these findings highlight that the efficiency of PMC/Co^{2+}-based AOPs can be highly sensitive to the background water matrix, where naturally occurring anions may either promote or inhibit radical production depending on their reactivity and interaction with Co^{2+}. This underscores the importance of evaluating real water systems, where multiple inorganic species coexist, to better predict the practical performance of PMC-driven oxidation processes.

3.3. Modelling kinetics of $^•OH$ formation

The overall chemical reaction of PMC formation from hydrogen peroxide and bicarbonate in aqueous solutions can be written as:

$$H_2O_2 + HCO_3^- \rightleftharpoons HCO_4^- + H_2O \qquad (R5)$$
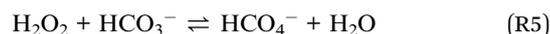
From a mechanistic perspective, E. V. Bakhmutova-Albert and co-workers[33] proposed that PMC forms via the reactions of hydrogen peroxide with dissolved carbon dioxide, $CO_{2,eq}$:
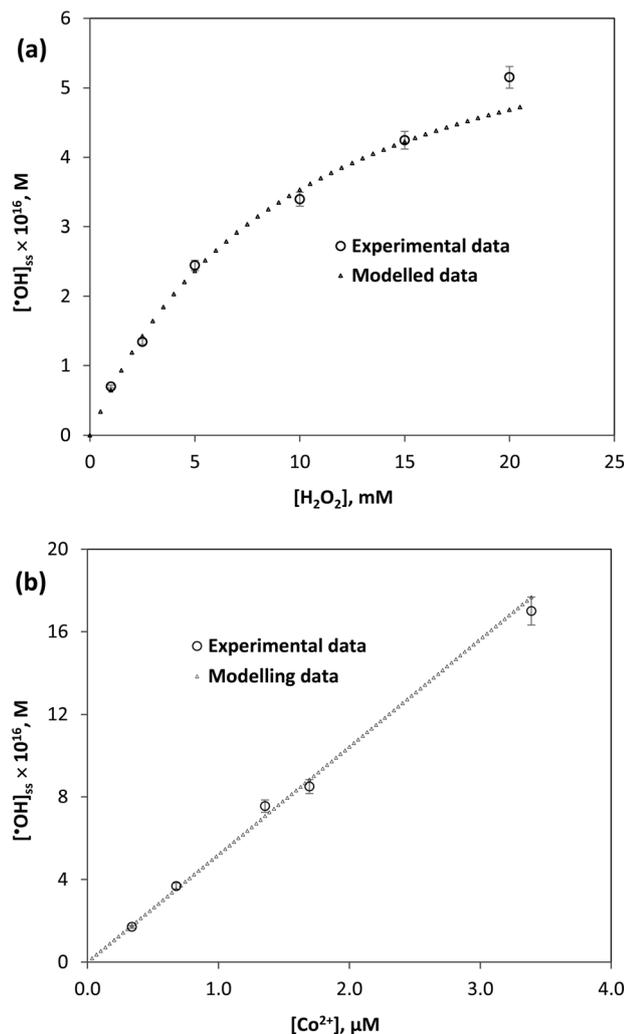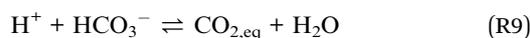
$$CO_{2,eq} + H_2O_2 \rightleftharpoons H_2CO_4 \qquad (R6)$$

$$H_2CO_4 \rightleftharpoons H^+ + HCO_4^- \qquad (R7)$$
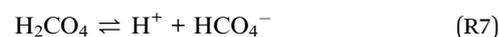
Fig. 7 Application of the $^{\bullet}$OH formation kinetic model to study the influence of the oxidant (a) and Co^{2+} catalyst (b) concentrations on the $^{\bullet}$OH concentration.

$$CO_{2,eq} + HO_2^- \rightleftharpoons HCO_4^- \tag{R8}$$

In which, $CO_{2,eq}$ is created by dehydrating of bicarbonate:

$$H^+ + HCO_3^- \rightleftharpoons CO_{2,eq} + H_2O \tag{R9}$$

Reactions (R6) ÷ (R8) are in equilibrium, the total concentration of PMC species can be established by:

$$[PMC]_{tot} = [H_2CO_4] + [HCO_4^-]$$
$$= K_{6,eq}[CO_{2,eq}][H_2O_2] + K_{8,eq}[CO_{2,eq}][HO_2^-] \tag{4}$$

where $[HO_2^-] = \alpha[H_2O_2]_{tot}$, and $[H_2O_2] = (1-\alpha)[H_2O_2]_{tot}$, with $[H_2O_2]_{tot}$ is the total concentration of hydrogen peroxide. Eqn (4) becomes:

$$[PMC] = \left(K_{6,eq}(1-\alpha) + \alpha K_{8,eq}\right)[CO_{2,eq}][H_2O_2]_{tot}$$
$$= K[CO_{2,eq}][H_2O_2]_{tot} \tag{5}$$

where $K = K_{6,eq}(1-\alpha) + \alpha K_{8,eq}$.

At a constant pH of the experiment (pH = 9), K will be a constant. We also assume that concentration of $CO_{2,eq}$ negligibly changes when bicarbonate concentration is changed in all experiments. Eqn (5) is modified to:

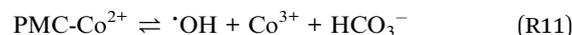$$[PMC] = a[H_2O_2]_{tot} \tag{6}$$

in which a is constant, $a = K[CO_{2,eq}]$.

In the presence of Co^{2+} ions, we postulate an equilibrium reaction form a highly reactive complex between PMC species and Co^{2+} as follows:

$$PMC + Co^{2+} \underset{k_{-10}}{\overset{k_{10}}{\rightleftharpoons}} PMC\text{-}Co^{2+} \tag{R10}$$

then it readily decomposes to create $^{\bullet}$OH radical:

$$PMC\text{-}Co^{2+} \rightleftharpoons {}^{\bullet}OH + Co^{3+} + HCO_3^- \tag{R11}$$

Co^{2+} can be regenerated by the reaction:

$$H_2O_2 + Co^{3+} \rightarrow HO_2^{\bullet} + Co^{2+} + H^+ \tag{R3}$$

It can be seen that steady-state concentration of $^{\bullet}$OH radical is proportional to PMC-Co^{2+} concentration, and can be written by:

$$[^{\bullet}OH]_{ss} = k[PMC\text{-}Co^{2+}] \tag{7}$$

Applying a steady-state aproximation for the complex PMC-Co^{2+}:

$$\frac{d[PMC\text{-}Co^{2+}]}{dt} = k_{10}[PMC][Co^{2+}] - k_{-10}[PMC\text{-}Co^{2+}]$$
$$- k_{11}[PMC\text{-}Co^{2+}]$$
$$= 0$$

with the initial Co^{2+} concentration: $[Co^{2+}]_{tot} = [Co^{2+}] + [PMC\text{-}Co^{2+}]$, we obtain:

Table 3 Comparison of the experimental and modelled values of $[^{\bullet}OH]_{ss}$ obtained with various concentrations of HCO_3^- : H_2O_2 mixture

No	$[HCO_3^-]$, mM	$[H_2O_2]$, mM	$[^{\bullet}OH]_{ss, exp.} \times 10^{16}$, M	$[^{\bullet}OH]_{ss, mod.} \times 10^{16}$, M	Difference %
1	0.4	1	0.70	0.65	6.9
2	1	2.5	1.32	1.43	7.9
3	2	5	2.31	2.36	2.4
4	4	10	3.68	3.53	4.0
5	6	15	4.11	4.23	2.9
6	8	20	5.15	4.70	8.7

Table 4 Comparison of the experimental and modelled values of $[\text{\textperiodcentered OH}]_{ss}$ obtained with various concentrations of Co^{2+} catalyst

No	$[Co^{2+}]$, μM	$[\text{\textperiodcentered OH}]_{ss, exp.} \times 10^{16}$, M	$[\text{\textperiodcentered OH}]_{ss, mod.} \times 10^{16}$, M	Difference, %
1	0.34	1.7	1.8	<5
2	0.68	3.7	3.5	<5
3	1.36	7.6	7.1	<7
4	1.69	8.5	8.8	<5
5	3.38	17.0	17.7	<5

$$[\text{PMC-Co}^{2+}] = \frac{[\text{PMC}][\text{Co}^{2+}]_{\text{tot}}}{[\text{PMC}] + \dfrac{(k_{-10} + k_{11})}{k_{10}}} = \frac{[\text{PMC}][\text{Co}^{2+}]_{\text{tot}}}{[\text{PMC}] + K_1} \quad (8)$$

where $K_1 = \dfrac{k_{-10} + k_{11}}{k_{10}}$. Inserting eqn (8) into (7) to obtain:

$$[\text{\textperiodcentered OH}]_{ss} = \frac{k[\text{Co}^{2+}][\text{PMC}]_{\text{tot}}}{[\text{PMC}] + K_1} \quad (9)$$

When $[\text{Co}^{2+}]_{\text{tot}}$ is kept the same for all experiments, eqn (9) becomes:

$$[\text{\textperiodcentered OH}]_{ss} = \frac{k'[\text{PMC}]}{[\text{PMC}] + K_1} \quad (10)$$

where $k' = k[\text{Co}^{2+}]_{\text{tot}}$.

Combining eqn (10) and (6) to obtain:

$$[\text{\textperiodcentered OH}]_{ss} = \frac{k'a[\text{H}_2\text{O}_2]_{\text{tot}}}{a[\text{H}_2\text{O}_2]_{\text{tot}} + K_1} = \frac{k'[\text{H}_2\text{O}_2]_{\text{tot}}}{[\text{H}_2\text{O}_2]_t + K_1/a} = \frac{k'[\text{H}_2\text{O}_2]_{\text{tot}}}{[\text{H}_2\text{O}_2]_t + K_1'}$$

with $K_1' = K_1/a$.

or

$$[\text{\textperiodcentered OH}]_{ss} = \frac{k[\text{Co}^{2+}]_{tot}[\text{H}_2\text{O}_2]_{\text{tot}}}{[\text{H}_2\text{O}_2]_{\text{tot}} + K_1'} \quad (11)$$

This proposed model reveals that steady-state formed $\text{\textperiodcentered OH}$ concentration is not linearly proportional to hydrogen peroxide concentration. The relationship has the form of Langmuir adsorption isotherm with a maximum concentration of $\text{\textperiodcentered OH}$ will be equal to $k[\text{Co}^{2+}]$ when increasing $[\text{H}_2\text{O}_2]$. Eqn (11) was fitted to experimental data by using Excel's Solver to get the value of k and K_1'. The optimization gives:

$$[\text{\textperiodcentered OH}]_{ss} = \frac{10.3 \times 10^{-16}[\text{Co}^{2+}][\text{H}_2\text{O}_2]_{\text{tot}}}{[\text{H}_2\text{O}_2]_{\text{tot}} + 0.0097}(\text{M}) \quad (12)$$

where $[\text{Co}^{2+}]$ in μmol L^{-1}, $[\text{H}_2\text{O}_2]$ in mol L^{-1}.

Applying this kinetic model to study the influence of the oxidant and Co^{2+} catalyst concentrations on the $\text{\textperiodcentered OH}$ formation, the results are presented in Fig. 7a, b and Tables 3, 4. It can be seen that the differences between modelled and experimental values are negligible (<9%), which reveals a good agreement. In other words, the kinetic model fitted well with the experimental results, thereby can be applied to evaluate the $\text{\textperiodcentered OH}$ steady-state concentration in the PMC/Co^{2+} systems.

4 Conclusions

In this work, $\text{\textperiodcentered OH}$ production in PMC-based AOPs was shown to be negligible without of a transition-metal catalyst but significantly enhanced in the presence of Co^{2+} through a Fenton-like mechanism. Quantitative analysis confirmed that steady-state $\text{\textperiodcentered OH}$ concentrations increased nearly 6-fold in H_2O_2/Co^{2+} compared to H_2O_2 alone, and over tenfold in PMC/Co^{2+} compared to PMC-alone systems. Kinetic investigations demonstrated first-order dependence on TA concentration, Langmuir-type behavior with oxidant concentration, and a linear relationship with Co^{2+} concentration, validating the proposed kinetic model. Inorganic anions modulated radical generation, with Cl^- promoting $\text{\textperiodcentered OH}$ formation and SO_4^{2-} and HPO_4^{2-} acting as inhibitors. These findings provide a mechanistic basis for understanding radical formation in PMC-based AOPs and underscore the importance of Co^{2+} catalyst and matrix composition in tuning $\text{\textperiodcentered OH}$ availability. The insights gained advance the fundamental knowledge of PMC-mediated oxidation systems and pave the way for their rational application in wastewater treatment and other environmental remediations.

Author contributions

Investigation, formal analysis, and methodology: Thi Tinh Vu. Supervision, validation, and writing – original draft: Thi Bich Viet Nguyen. Supervision and writing – review & editing: Ngoc Duy Vu.

Conflicts of interest

There are no conflicts to declare.

Data availability

References

1 Y. Liu and J. Wang, *Chem. Eng. J.*, 2023, **466**, 143147, DOI: **10.1016/j.cej.2023.143147**.

2 M. Mahmoodi and E. Pishbin, *Environ. Sci. Pollut. Res.*, 2025, **32**, 3531–3570, DOI: **10.1007/s11356-024-35835-w**.

3 E. H. Khader, S. A. Muslim, N. M. Cata Saady, N. S. Ali, I. K. Salih, T. J. Mohammed, T. M. Albayati and S. Zendehboudi, *Desalin. Water Treat.*, 2024, **318**, 100384, DOI: **10.1016/j.dwt.2024.100384**.

4 R. El Asmar, A. Baalbaki, Z. Abou Khalil, S. Naim, A. Bejjani and A. Ghauch, *Chem. Eng. J.*, 2021, **405**, 126701, DOI: **10.1016/j.cej.2020.126701**.

5 T. B. V. Nguyen, N. Nguyen-Bich, N. D. Vu, H. Ho Phuong and H. Nguyen Thi, *J. Anal. Methods Chem.*, 2021, **2021**, 6696600, DOI: **10.1155/2021/6696600**.

6 T. H. Nguyen, T. H. Pham, H. T. Nguyen, B. N. Nguyen, N. D. Vu and T. B. V. Nguyen, *Vietnam J. Chem.*, 2022, **60**, 96, DOI: **10.1002/vjch.202200089**.

7 H. Pan, Y. Gao, N. Li, Y. Zhou, Q. Lin and J. Jiang, *Chem. Eng. J.*, 2020, **408**, 2021, DOI: **10.1016/j.cej.2020.127332**.

8 N. A. Urbina-Suarez, C. Rivera-Caicedo, Á. D. González-Delgado, A. F. Barajas-Solano and F. Machuca-Martínez, *Toxics*, 2023, **11**, 366, DOI: **10.3390/toxics11040366**.

9 K. Y. Mora-Bonilla, I. F. Macías-Quiroga, N. R. Sanabria-González and M. T. Dávila-Arias, *ChemEngineering*, 2023, **7**(5), 86, DOI: **10.3390/chemengineering7050086**.

10 J. L. Wang and l. J. Xu, *Crit. Rev. Environ. Sci. Technol.*, 2012, **42**(3), 251, DOI: **10.1080/10643389.2010.507698**.

11 G. V. Buxton, C. L. Greenstock, W. P. Helamn and A. B. Ross, *J. Phys. Chem. Ref. Data*, 1988, **17**, 513–886, DOI: **10.1063/1.555805**.

12 Y. Nosaka and A. Y. Nosaka, *Chem. Rev.*, 2017, **117**, 11302, DOI: **10.1021/acs.chemrev.7b00161**.

13 E. Finkelstein, G. M. Rosen and E. J. Rauckman, *Arch. Biochem. Biophys.*, 2022, **726**, 109191, DOI: **10.1016/0003-9861(80)90323-9**.

14 Z. R. Lin, L. Zhao and Y. H. Dong, *Chemosphere*, 2015, **141**, 7, DOI: **10.1016/j.chemosphere.2015.05.066**.

15 Y. Zuo, *Chemosphere*, 2003, **51**(3), 175, DOI: **10.1016/S0045-6535(02)00803-2**.

16 A. A. Dalle, L. Dmergue, F. Fourcade, A. A. Assadi, H. Djelal, T. Lendormi, I. Soutrel, S. Taha and A. Amrane, *Electrochim. Acta*, 2017, **246**, 1, DOI: **10.1016/j.electacta.2017.06.024**.

17 K. Takeda, H. Takedoi, S. Yamaji, K. Ohta and H. Sakugawa, *Anal. Sci.*, 2004, **20**, 153, DOI: **10.2116/analsci.20.153**.

18 M. Ahmad, A. L. Teel, O. S. Furman, J. I. Reed and R. J. Watts, *J. Environ. Eng.*, 2012, **138**, 411, DOI: **10.1061/(ASCE)EE.1943-7870.0000496**.

19 F. Sun, T. Chen, X. Zou, H. Liu, Z. Chu, D. Shu, H. Wang, F. Huang and D. Chen, *Appl. Geochem.*, 2021, **126**, 104893, DOI: **10.1016/j.apgeochem.2021.104893**.

20 B. Bektaşoğlu, Mustafa Özyürek, Kubilay Güçlü, Reşat Apak, *Talanta*, 2008, **77**(1), 90–97, DOI: **10.1016/j.talanta.2008.05.043**.

21 S. C. Fisher, M. A. A. Schoonen and B. J. Brownawell, *Geochem. Trans.*, 2012, **13**, 3, DOI: **10.1186/1467-4866-13-3**.

22 S. Backa, K. Jansbo and T. Reitberger, *Holzforschung*, 1997, **51**, 557–564.

23 Y. Pi, J. Schmacher and M. Jekel, *Ozone: Sci. Eng.*, 2005, **27**(6), 431, DOI: **10.1080/01919510500349309**.

24 S. E. Page, W. A. Arnold and K. McNeill, *J. Environ. Monit.*, 2010, **12**, 1658, DOI: **10.1039/c0em00160k**.

25 M. Saran and K. H. Summer, *Free Radic. Res.*, 1999, **31**(5), 429, DOI: **10.1080/10715769900300991**.

26 T. Charbouillot, M. Brigantea, G. Mailhot, P. R. Maddigapu, C. Minero and D. Vione, *J. Photochem. Photobiol., A*, 2011, **222**, 70, DOI: **10.1016/j.jphotochem.2011.05.003**.

27 D. H. Gonzalez, X. M. Kuang, J. A. Scott, G. O. Rocha and S. E. Paulson, *Anal. Lett.*, 2018, **51**(15), 2488–2497, DOI: **10.1080/00032719.2018.1431246**.

28 T. Tinh Vu and T. B. Viet Nguyen, *HNUE J. Sci. Nat. Sci.*, 2024, **69**(3), 96, DOI: **10.18173/2354-1059.2024-0039**.

29 J. J. Pignatello, E. Oliveros and A. MacKay, *Crit. Rev. Environ. Sci. Technol.*, 2006, **36**, 1, DOI: **10.1080/10643380500326564**.

30 U. von Gunten, *Water Res.*, 2003, **37**, 1443, DOI: **10.1016/S0043-1354(02)00457-8**.

31 P. Neta and R. E. Huie, *J. Phys. Chem. Ref. Data*, 1986, **15**, 1027, DOI: **10.1063/1.555808**.

32 S. Canonica and U. von Gunten, *Water Sci. Technol.*, 2007, **55**(12), 125, DOI: **10.1021/es025896h**.

33 E. V. Bakhmutova-Albert, H. Yao, D. E. Denevan and D. E. Richardson, *Inorg. Chem.*, 2010, **49**, 11287, DOI: **10.1021/ic1007389**.